Biochemical Pharmacology 79 (2010) 431–443

Contents lists available at ScienceDirect

Biochemical Pharmacology

journal homepage: www.elsevier.com/locate/biochempharm

Src-mediated regulation of inflammatory responses by actin polymerization

Joo Young Kim [a,1], Yong Gyu Lee [a,1], Mi-Yeon Kim [b], Se Eun Byeon [a], Man Hee Rhee [c], Jongsun Park [d], David R. Katz [e], Benjamin M. Chain [e], Jae Youl Cho [a,*]

[a] School of Bioscience and Biotechnology, and Institute of Bioscience and Biotechnology, Kangwon National University, 192-1 Hyoja-2-Dong, Chuncheon 200-701, Republic of Korea
[b] Department of Bioinformatics and Life Science, Soongsil University, Seoul 156-743, Republic of Korea
[c] College of Veterinary Medicine, Kyungpook National University, Daegu 702-701, Republic of Korea
[d] Department of Pharmacology, Daejeon Regional Cancer Center, Cancer Research Institute, College of Medicine, Chungnam National University, Daejeon 310-010, Republic of Korea
[e] Department of Immunology and Molecular Pathology, UCL, Windeyer Building, 46 Cleveland St., London, W1T 4JF, UK

ARTICLE INFO

Article history:
Received 16 July 2009
Accepted 14 September 2009

Keywords:
Actin cytoskeleton
Inflammation
Cytochalasin B
Src kinase
NF-κB

ABSTRACT

Although the role of the actin cytoskeleton has become increasingly elucidated, the role of actin polymerization in inflammatory processes remains poorly understood. Here, we examine the role of the actin cytoskeleton during LPS-mediated inflammatory events in RAW264.7 cells and peritoneal macrophages. We observed that actin cytoskeleton disruption by cytochalasin B and siRNA to cytoplasmic actin strongly down-regulated LPS-mediated inflammatory responses such as NO production, PGE_2 release, and TNF-α secretion. Actin cytoskeleton disruption by cytochalasin B down-regulated a series of signaling cascades including PI3K, Akt, and IKK, but not MAPKs, necessary for NF-κB activation without down-regulating total forms of the proteins as assessed by measuring their phosphorylation levels. In particular, cytochalasin B significantly inhibited LPS-induced both phosphorylation and kinase activity of Src without altering total level, implying that Src may be a potential pharmacological target of actin cytoskeleton rearrangement. Moreover, the direct association of Src with actin was actin polymerization-dependent according to immunoprecipitation analysis performed with a GFP-actin wild type and HA-tagged Src. Therefore, our data suggest that actin cytoskeleton rearrangement may be a key event during the regulation of inflammatory responses that modulates the activity of Src and its downstream signaling molecules.

1. Introduction

Chronic (or acute) inflammation is a multiple step process that is mediated by activated inflammatory or immune cells. Of these, macrophages play a central role in managing many different immunopathological phenomena during inflammation, such as the over-production of inflammatory mediators [nitric oxide (NO) and prostaglandin E_2 (PGE_2)], which are generated by activated inducible nitric oxide synthase (iNOS) and cyclooxygenase (COX)-2 [1,2]. These cellular events are mainly managed by surface receptors [pattern recognition receptor (PRR)] such as the toll-like receptors (TLR)-4 or TLR-2 [3]. Activation of these molecules by some inflammatory stimuli such as lipopolysaccharide (LPS) in macrophages up-regulates intracellular signaling machinery, including mitogen activated protein kinases (MAPKs) and non-receptor type tyrosine kinases, up-regulating inflammatory gene expression via activation of transcription factors such as the nuclear factor (NF)-κB and activator protein (AP)-1 [4,5]. Primary macrophages and cancerous macrophage-like cells (e.g., RAW264.7 and J774 cells) induced by LPS are now regarded as a useful *in vitro* model for evaluating the potency of anti-inflammatory drugs as well as exploring their anti-inflammatory mechanisms, due to their ability to display similar inflammatory states [6].

Actin filaments make up one of the major cytoskeleton systems of the cell. The actin cytoskeleton plays an important role in modulating cell morphology (e.g., fillopodia), villi formation, cell division via contractile ring formation, cell migration, and intracellular signaling pathways [7,8]. Although various roles of actin filaments in various cellular responses have been reported, their functions in macrophages during inflammatory responses are not well understood. The actin cytoskeleton is known to modulate the migration and adhesion of monocytes and macrophages. Disruption of the actin cytoskeleton with angiostatin, therefore, leads to suppression of macrophage migration [9]. Actin cytoskeleton rearrangement is clearly seen during microbial infection of macrophages and sequential formation of the

* Corresponding author. Tel.: +82 33 250 6488; fax: +82 33 242 6480.
E-mail address: jaecho@kangwon.ac.kr (J.Y. Cho).
[1] These authors equally contributed.

0006-2952/$ – see front matter © 2009 Elsevier Inc. All rights reserved.
doi:10.1016/j.bcp.2009.09.016

endosome/phagosome via Fc receptor-dependent or -independent mechanisms [10,11]. There is also evidence that the actin cytoskeleton plays a critical role in the stimulation of cholesterol esterification by atherogenic lipoproteins in macrophages [12]. The actin cytoskeleton is also reported to modulate inflammatory gene expression. Thus, disruption of the actin cytoskeleton potentiated IL-1β-induced iNOS expression in rat mesangial cells [13], while iNOS expression in macrophages is tightly associated with the cytoskeletal protein α-actinin 4, suggesting that cellular localization and interaction of iNOS with the cytoskeleton is required for enzyme function [14]. LPS-induced TNF-α production and COX-2 expression are also known to require cytochalasin-sensitive actin cytoskeleton rearrangement, which is sensitive to ethanol treatment [15,16]. Although these reports indicate a functional role for the actin cytoskeleton in various macrophage functions, the molecular events associated with how the actin cytoskeleton modulates various cellular responses remain unclear. Currently, Rho family protein (Rac2), ERK, p38, PI3K, Akt, Syk, and NF-κB were found to be regulating components linked to the actin cytoskeleton [17–19].

Based on previous reports [15,16], several issues such as whether actin reorganization plays a critical role in modulating macrophage responses to various inflammatory stimuli, whether the actin filament modulates the activation of transcription factors that regulate inflammatory gene control, and whether the actin cytoskeleton is selectively linked to a specific intracellular signaling component involved in inflammatory signaling events were raised to be addressed. The aim of the present study, therefore, was to demonstrate the regulatory role of the actin cytoskeleton during inflammatory responses of macrophages under LPS exposure. We also explored the regulatory mechanisms of the actin cytoskeleton in terms of intracellular signaling, and the molecular interaction between actin and its associated molecules.

2. Materials and methods

2.1. Materials

Cytochalasin B (from *Helminthosporium dematioideum*), peptidoglycan, curdlan, zymosan A, paclitaxel (from *Taxus brevifolia*, a tubulin disassembly inhibitor: Baccatin III N-benzyl-β-phenylisoserine Ester), sulfanilamide, N-[1-naphthyl]-ethylenediamine dihydrochloride, phosphoric acid, phorbol 12-myristate 13-acetate (PMA), siRNA to cytoplasmic actin, negative control RNA, tumor necrosis factor (TNF)-α, and lipopolysaccharide (LPS, *Escherichia coli* 0111:B4) were purchased from Sigma Chemical Co. (St. Louis, MO). PP2 (a Src family kinase inhibitor: 4-amino-5-(4-chlorophenyl)-7-(t-butyl)pyrazolo[3,4-d]pyramidine), colchicines (a disruption agent of microtubules and tubulin polymerization inhibitor), BTS (a myosin S1 inhibitor), latrunculin B (an actin polymerization inhibitor) were obtained from Calbiochem (La Jolla, CA). IFN-γ was obtained from Biovision (Mountain View, CA). Rhodamine phalloidin was purchased from Molecular Probes (Carlsbad, CA). Fetal bovine serum and RPMI1640 were obtained from GIBCO (Grand Island, NY). RAW264.7 and HEK293 cells were purchased from the American Tissue Culture Center (Rockville, MD). TLR4-expressing-HEK293 cells were a kind gift from Prof. Katherine A. Fitzgerald (University of Massachusetts Medical School, Worcester, MA). Vector containing a GFP-fused cytosolic full length actin gene (pAcGFP1-Actin) was purchased from Clonetech (Mountain View, CA). Luciferase construct containing NF-κB binding promoters was gifts from Prof. Chung, Hae Young (Pusan National University, Pusan, Korea). All other chemicals were of Sigma grade. Anti-GFP and HA antibodies were purchased from Santa Cruz Biotechnology (Santa Cruz, CA). Phospho- or total-antibodies to Akt, Src, p85, ERK, p38, JNK, IKKβ and IκBα were purchased from Cell Signaling (Beverly, MA). Alexa 488-conjugated secondary antibody was obtained from Invitrogen (Carlsbad, CA).

2.2. Construction of expression vectors

GFP-fused wild type actin construct (GFP-actin-WT) was prepared by amplification using a typical culture method with competent *E. coli* (DH5α). pcDNA-HA, and pcDNA-HA-tagged c-Src construct (Src-WT) were the same as reported previously [20].

2.3. Preparation of peritoneal macrophages

C57BL/6 male mice (6–8 weeks old, 17–21 g) were obtained from DAEHAN BIOLINK (Chungbuk, Korea) and maintained in plastic cages under conventional conditions. Water and pelleted diets (Samyang, Daejeon, Korea) were supplied ad libitum. Studies were performed in accordance with guidelines established by the Kangwon National University Institutional Animal Care and Use Committee. Peritoneal exudates were obtained from C57BL/6 male mice (6–8 weeks old, 17–21 g) by lavaging 4 days after intraperitoneal injection of 1 ml of sterile 4% thioglycollate broth (Difco Laboratories, Detroit, MI). Washed cells were resuspended in RPMI 1640 medium containing 10% FBS and plated in 60-mm tissue culture dishes for 4 h at 37 °C in a 5% CO_2 humidified atmosphere to prepare peritoneal macrophages.

2.4. Cell culture

Peritoneal macrophage and RAW264.7 cells were maintained in RPMI1640 and wild type HEK293 and TLR4-expressing HEK293 cells were cultured in DMEM. Both mediums were also supplemented with 100 U/ml of penicillin, 100 μg/ml of streptomycin, and 10% fetal bovine serum. Cells were grown at 37 °C with 5% CO_2.

2.5. Determination of NO, PGE_2, and TNF-α production

RAW 264.7 cells (1×10^6 cells/ml) under normal culture conditions were preincubated with each compound for 30 min and continuously activated with LPS (2 μg/ml) for 24 h [21]. The nitrite in culture supernatants was also measured by adding 100 μl of Griess reagent (1% sulfanilamide and 0.1% N-[1-naphthyl]-ethylenediamine dihydrochloride in 5% phosphoric acid) to 100 μl of sample medium for 10 min at room temperature. The OD at 570 nm (OD_{570}) was measured using a Spectramax 250 microplate reader (Molecular Devices, Sunnyvale, CA, USA). A standard curve for NO was made with sodium nitrite. The detection limit of the assay was 0.5 μM.

The inhibitory effects of cytochalasin B on PGE_2 and TNF-α production in LPS-treated RAW264.7 cells (1×10^6 cells/ml) was determined as described previously [22]. RAW 264.7 cells (1×10^6 cells/ml) were preincubated with cytochalasin B for 30 min and continuously activated with LPS (2 μg/ml) for 24 h (PGE_2) or 6 h (TNF-α). Supernatants were harvested and assayed for PGE_2 and TNF-α using the EIA and ELISA kits (Amersham, Little Chalfont, Buckinghamshire, UK).

2.6. mRNA detection by quantitative and semi-quantitative real-time reverse transcription-PCR

Total RNA from LPS-treated-RAW264.7 cells (5×10^6 cells/ml) was prepared by adding TRIzol Reagent (Gibco BRL) according to the manufacturer's protocol. The total RNA solution was stored at −70 °C until used. Semi-quantitative RT reactions were conducted using MuLV reverse transcriptase. Total RNA (1 μg) was incubated with oligo-dT15 for 5 min at 70 °C and mixed with a 5× first-strand buffer, 10 mM dNTPs, and 0.1 M DTT. The reaction mixture was

further incubated for 5 min at 37 °C and for 60 min after the addition of MuLV reverse transcriptase (2 U). Reactions were terminated after 10 min at 70 °C, and total RNA was depleted by adding RNase H. The PCR reaction was conducted with the incubation mixture (2 μl cDNA, 4 μM 5′ and 3′ primers, a 10× buffer [10 mM Tris–HCl, pH 8.3, 50 mM KCl, 0.1% Triton X-100], 250 μM of dNTP, 25 mM of $MgCl_2$, and 1 unit of Taq polymerase [Promega, USA]). The following incubation conditions were used: a 30 s denaturation time at 94 °C, an annealing time of 30 s between 55 and 60 °C, an extension time of 45 s at 72 °C, and a final extension of 5 min at 72 °C. For real-time PCR analysis, 1 μg of RNA was submitted to reverse transcription with the Molony murine leukemia virus reverse transcriptase (Invitrogen). Two microliters of cDNA obtained for each sample were submitted to a qPCR using the SYBR green Master mix method (Applied Biosystems, Foster City, CA) in the ABO sequence detection system. The results were normalized with the 18S transcript. The primers (Bioneer, Daejeon, Korea) used in this experiment are indicated in Table 1.

2.7. Luciferase reporter gene activity assay

HEK293 and TLR4-expressing-HEK cells (1×10^6 cells/ml) were transfected with 1 μg of plasmids containing NF-κB-Luc, or AP-1-Luc as well as β-galactosidase using the calcium phosphate method in a 12-well plate according to the manufacturer's protocol. The cells were used for experiments 48 h after transfection. Luciferase assays were performed using the Luciferase Assay System (Promega) [23]. Briefly, transfected cells treated with cytochalasin B in the presence of PMA (10 ng/ml) and TNF-α (20 ng/ml) or LPS (2 μg/ml) were lysed in culture dishes with reporter lysis buffer. Lysates were centrifuged at maximum speed for 10 min in an Eppendorf microcentrifuge. Fifty microliters of the supernatant fraction was incubated with 50 μl of luciferase substrate, and the relative luciferase activity was determined with a Luminoskan Ascent (Thermo Labsystems Oy, Helsinki, Finland). Luciferase activity was normalized to β-galactosidase activity, measured at 405 nm, by enzymatic reaction with X-gal and lysate for 5 min at 37 °C.

2.8. Confocal microscopy for surface molecules

RAW264.7 cells were plated at a density of 2×10^5 cells/well in 12-well plates containing sterile cover slips and grown at 37 °C for 12 h. Cells were treated with cytochalasin B for 30 min, followed by stimulation with LPS (2 μg/ml) for 2 min. After treatment, the cells were washed twice with PBS prewarmed to 37 °C and fixed to the cover slips by incubating in 3.7% formaldehyde for 10 min. Cells were then washed three times with PBS. The coverslips were blocked in 1% BSA for 1 h at room temperature with shaking. CD14 (directly labeled FITC, rmC5-3, 1:50) antibody was added in 1% BSA and incubated for 1 h with shaking at room temperature. Antibodies to MD2 and phospho-Src were added in 1% BSA and incubated for 1 h with shaking. For cytoskeleton staining, rhodamine phalloidin (Molecular Probes, 1:250) was added in 1% BSA and incubated for 1 h in the dark. Coverslips were then washed three times each with PBS. Alexa 488-conjugated secondary antibody (1:100) was then added in 1% BSA and incubated for 1 h with shaking at room temperature. Coverslips were washed three times with PBS and mounted onto slides using Fluorescent mounting medium (DakoCytomation, Carpentaria, CA). Intensity changes in phospho-Src, CD14, MD2, and the cytoskeleton were imaged with an Olympus LX70 FV300 (Olympus, Tokyo, Japan) in the Central Laboratory of Kangwon National University.

Table 1
Primers used for quantitative real-time and semi-quantitative RT-PCR analyses.

Gene		Primer sequences
For semi-quantitative RT-PCR		
TNF-α	F	5′-TTGACCTCAGCGCTGAGTTG-3′
	R	5′-CCTGTAGCCCACGTCGTAGC-3′
COX-2	F	5′-CACTACATCCTGACCCACTT-3′
	R	5′-ATGCTCCTGCTTGAGTATGT-3′
iNOS	F	5′-CCCTTCCGAAGTTTCTGGCAGCAGC-3′
	R	5′-GGCTGTCAGAGCCTCGTGGCTTTGG-3′
GAPDH	F	5′-CACTCACGGCAAATTCAACGGCAC-3′
	R	5′-GACTCCACGACATACTCAGCAC-3′
For quantitative real-time RT-PCR		
TNF-α	F	5′-TGCCTATGTCTCAGCCTCTTC-3′
	R	5′-GAGGCCATTTGGGAACTTCT-3′
COX-2	F	5′-GGGAGTCTGGAACATTGTGAA-3′
	R	5′-GCACATTGTAAGTAGGTGGACTGT-3′
iNOS	F	5′-GGAGCCTTTAGACCTCAACAGA-3′
	R	5′-TGAACGAGGAGGGTGGTG-3′
GAPDH	F	5′-CAATGAATACGGCTACAGCAAC-3′
	R	5′-AGGGAGATGCTCAGTGTTGG-3′

F: forward, R: reverse.

2.9. Preparation of cell lysates and nuclear fraction, and immunoblotting

RAW264.7 cells (5×10^6 cells/ml) were washed 3 times in cold PBS with 1 mM sodium orthovanadate and lysed in lysis buffer (20 mM Tris–HCl, pH 7.4, 2 mM EDTA, 2 mM ethyleneglycotetraacetic acid, 50 mM β-glycerophosphate, 1 mM sodium orthovanadate, 1 mM dithiothreitol, 1% Triton X-100, 10% glycerol, 10 μg/ml aprotinin, 10 μg/ml pepstatin, 1 mM benzimide, and 2 mM PMSF) for 30 min with rotation at 4 °C. The lysates were clarified by centrifugation at 16,000 × *g* for 10 min at 4 °C and stored at −20 °C until needed.

Nuclear lysates were prepared with a three-step procedure [24]. After treatment, cells were collected with a rubber policeman, washed with 1× PBS, and lysed in 500 μl of lysis buffer containing 50 mM KCl, 0.5% Nonidet P-40, 25 mM HEPES (pH 7.8), 1 mM phenylmethylsulfonyl fluoride, 10 μg/ml leupeptin, 20 μg/ml aprotinin, and 100 μM 1,4-dithiothreitol (DTT) on ice for 4 min. Cell lysates were then centrifuged at 14,000 rpm for 1 min in a microcentrifuge. In the second step, the pellet (the nuclei fraction) was washed once in washing buffer, which was the same as the lysis buffer without Nonidet P-40. In the final step, nuclei were treated with an extraction buffer containing 500 mM KCl, 10% glycerol, and several other reagents as in the lysis buffer. The nuclei/extraction buffer mixture was frozen at −80 °C, and then thawed on ice and centrifuged at 14,000 rpm for 5 min. Supernatant was collected as nuclear extract.

Whole cell or nuclear lysates were then analyzed by immunoblotting. Proteins were separated on 10% SDS-polyacrylamide gels and transferred by electroblotting to polyvinylidenedifluoride (PVDF) membrane. Membranes were blocked for 60 min in Tris-buffered saline containing 3% bovine serum albumin, 20 mM NaF, 2 mM EDTA, and 0.2% Tween 20 at room temperature. The membrane was incubated for 60 min with specific primary antibody at 4 °C, washed 3 times with the same buffer, and incubated for an additional 60 min with HRP-conjugated secondary antibody. The total and phosphorylated levels of ERK, p38, JNK, IκBα, IKKβ, p85, Akt, Src, γ-tublin, cytoplasmic actin (actin) and β-actin were visualized using the ECL system (Amersham, Little Chalfont, Buckinghamshire, UK).

2.10. Immunoprecipitation and in vitro Src kinase activity assay

Cell lysates containing equal amounts of protein (500 μg) from RAW264.7 cells (1×10^7 cells/ml) treated with or without

LPS (2 μg/ml) for 3.5 min were precleared with 10 μl of protein A-coupled Sepharose Magnetic beads (50%, v/v) (ELPIS BIOTECH, Daejeon, Korea) for 1 h at 4 °C. Precleared samples were incubated with 5 μl of anti-Src antibody overnight at 4 °C. Immune complexes were mixed with 10 μl of protein A-coupled Sepharose Magnetic beads (50%, v/v) and rotated for 3 h at 4 °C. The immunoprecipitates were then washed three times with Src kinase reaction buffer [100 mM Tris–HCl, pH 7.2, 125 mM $Mg(C_2H_3O_2)_2$, 25 mM $MnCl_2$, 2 mM EGTA, 0.25 mM sodium orthovanadate, and 2 mM dithiothreitol], and reactions were carried out using components of a commercially available Src kinase assay kit (Upstate Biotechnology, Inc., Lake Placid, NY) according to the manufacturer's protocol. The assay is based on Src-dependent phosphorylation of a substrate peptide (KVEKIGEGTYGVVYK) derived from p34cdc2.

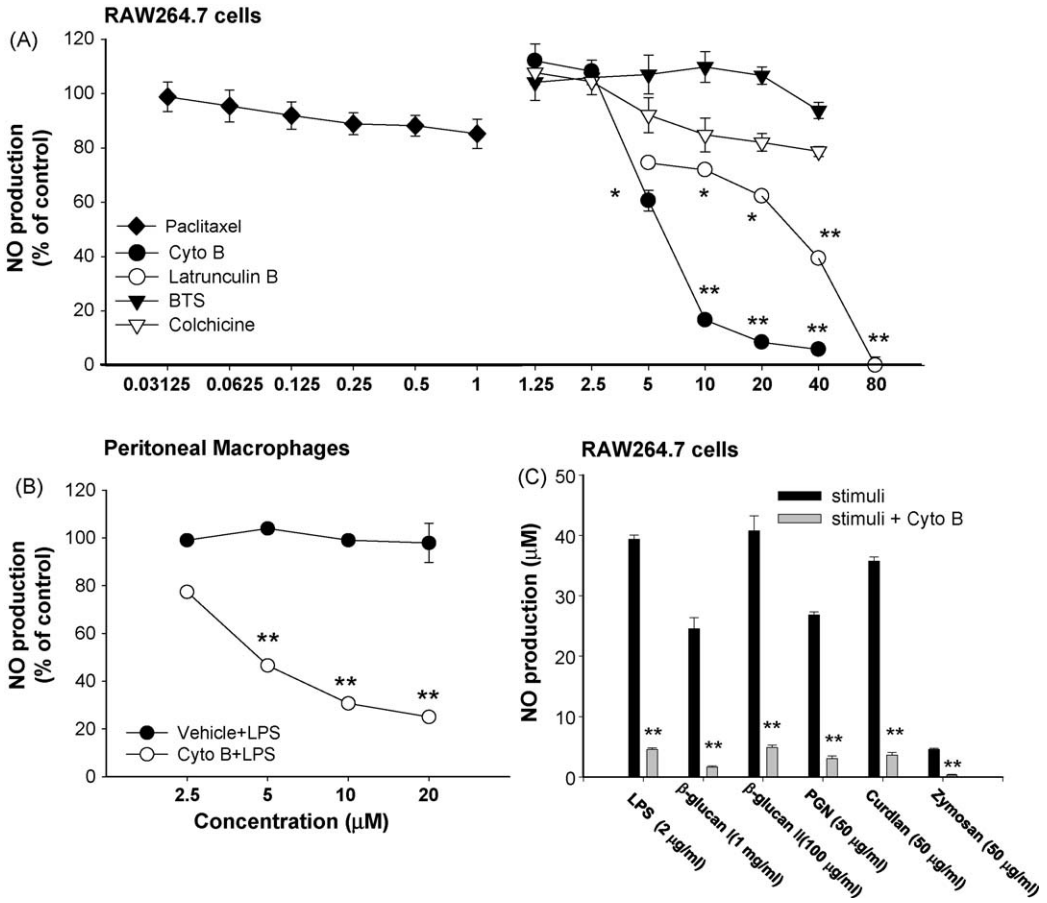

Fig. 1. The effects of cytoskeleton regulators on NO release from RAW264.7 cells or primary peritoneal macrophages treated with various inflammatory stimuli. (A) RAW264.7 cells (1×10^6 cells/ml) were incubated with cytochalasin B, paclitaxel, latrunculin B, colchicines, and BTS (N-benzyl-p-toluene sulfonamide) for 24 h. (B) Peritoneal macrophages (1×10^6 cells/ml) were incubated with cytochalasin B in the presence of LPS (2 μg/ml) for 24 h. (C) RAW264.7 cells (1×10^6 cells/ml) pre-treated with cytochalasin B were incubated with various inflammatory stimuli for 24 h. Supernatants were collected and the NO concentration in the supernatants was determined using Griess reagent. Data represent the mean ± SEM of three independent experiments performed in triplicate. $^*p < 0.05$ and $^{**}p < 0.01$ compared to the control group.

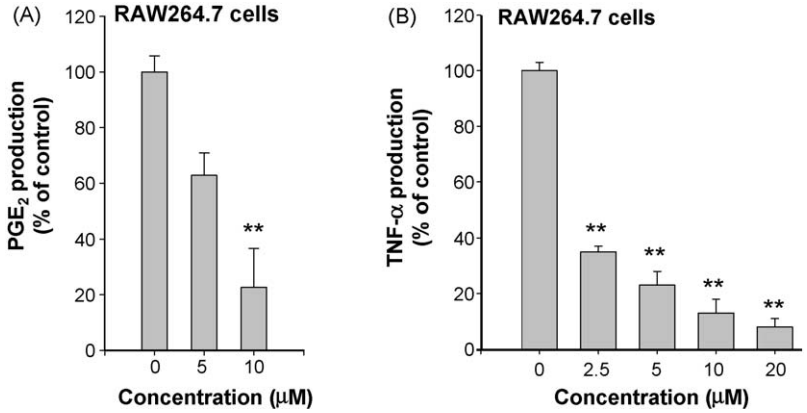

Fig. 2. The effect of cytochalasin B on PGE_2 production and TNF-α secretion from LPS-treated RAW264.7 cells. (A and B) RAW264.7 cells (1×10^6 cells/ml) were treated with cytochalasin B in the presence or absence of LPS (2 μg/ml) for 6 (TNF-α) or 24 (PGE_2) h. Supernatants were collected and PGE_2 and TNF-α levels present in the supernatants were determined by EIA (A) or ELISA (B) as described in Section 2. Data represent the mean ± SEM of three independent experiments performed in triplicate. $^{**}p < 0.01$ compared to the control group.

2.11. Statistical analysis

A Student's *t*-test and one-way ANOVA were used to determine the statistical significance of differences between values for the various experimental and control groups. Data are expressed as means ± standard errors (SEM) and the results were obtained from at least three independent experiments performed in triplicate. *P* values of 0.05 or less were considered as statistically significant.

3. Results

3.1. Involvement of the actin cytoskeleton in LPS-induced NO production

To address whether NO production from LPS-activated macrophages was selectively modulated by actin polymerization, various cytoskeleton modulators were evaluated using a macrophage-like cell line, RAW264.7 cells. As shown in Fig. 1A, cytochalasin B, an actin polymerization inhibitor, dose-dependently inhibited the production of NO in LPS-activated RAW264.7 cells with an IC_{50} value of 4.7 μM. Similarly, another disruptor of the actin cytoskeleton, latrunculin B, dose-dependently diminished NO release under the same conditions. However, other modulators such as paclitaxel (a tubulin disassembly inhibitor), colchicines (a disruption agent of microtubules and tubulin polymerization inhibitor), and BTS (a myosin S1 inhibitor) showed weak or no inhibitory activities. Cytochalasin B as well as other inhibitors did not affect the normal viability of RAW264.7 cells (Fig. S1).

To evaluate whether the effect of cytochalasin B was limited to the macrophage cell line, primary peritoneal macrophages were prepared and the NO inhibitory activity of cytochalasin B was

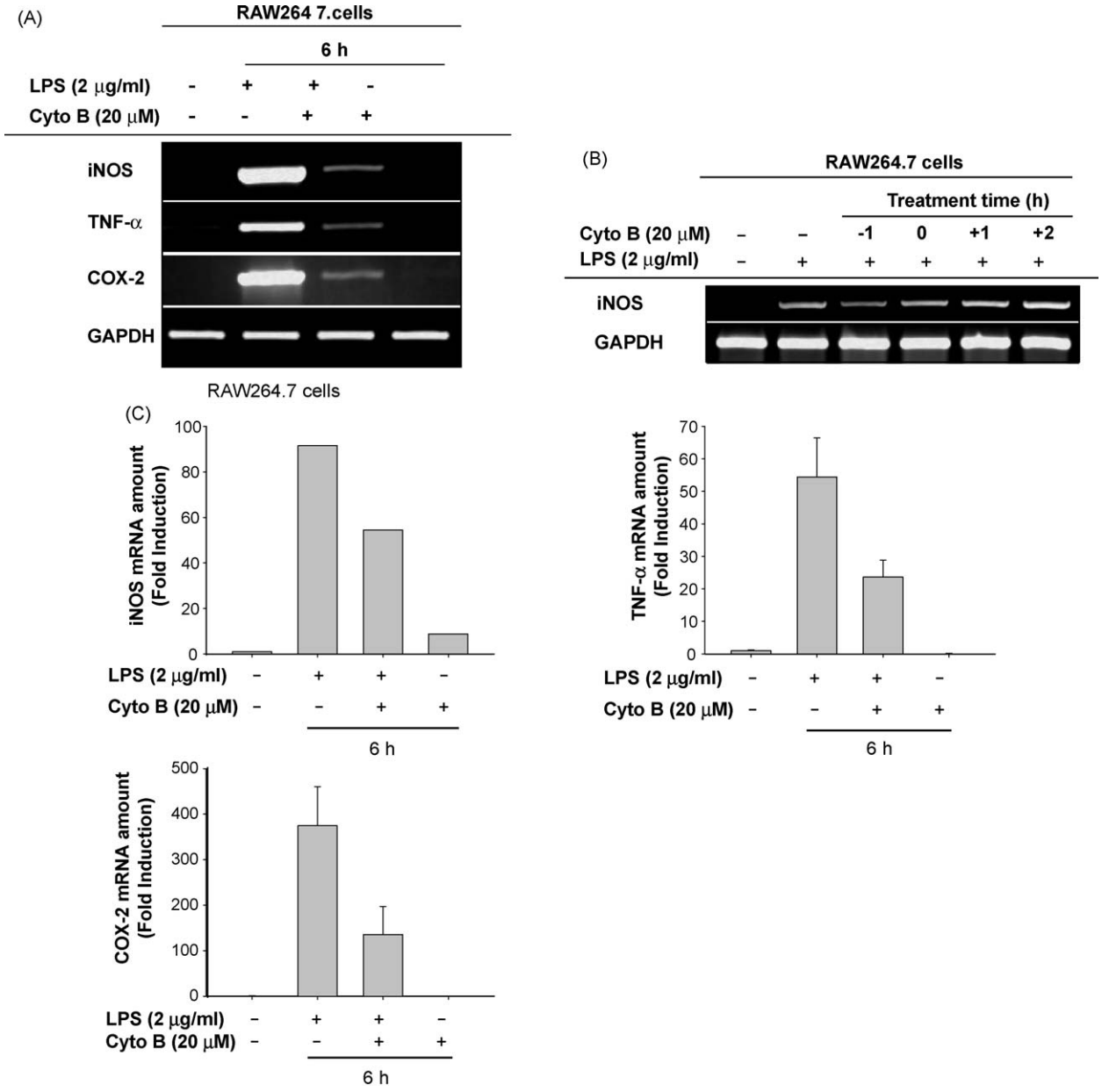

Fig. 3. The effect of cytochalasin B on the mRNA expression of iNOS, COX-2, and TNF-α in LPS-treated RAW264.7 cells. (A) RAW264.7 cells (5×10^6 cells/ml) were incubated with cytochalasin B in the presence or absence of LPS (2 μg/ml) for 6 h. (B) RAW264.7 cells (5×10^6 cells/ml) were treated with cytochalasin B 1 h prior to LPS (2 μg/ml), same time and 1 or 2 h after, and further incubated for 3 h. The mRNA levels of iNOS, COX-2, and TNF-α were determined by semi-quantitative RT-PCR (A and B). (C) mRNA levels of iNOS, COX-2, and TNF-α prepared from cytochalasin B-treated RAW264.7 cells in the presence or absence of LPS (2 μg/ml) were analyzed by quantitative real-time PCR. The results show one representative experiment of three.

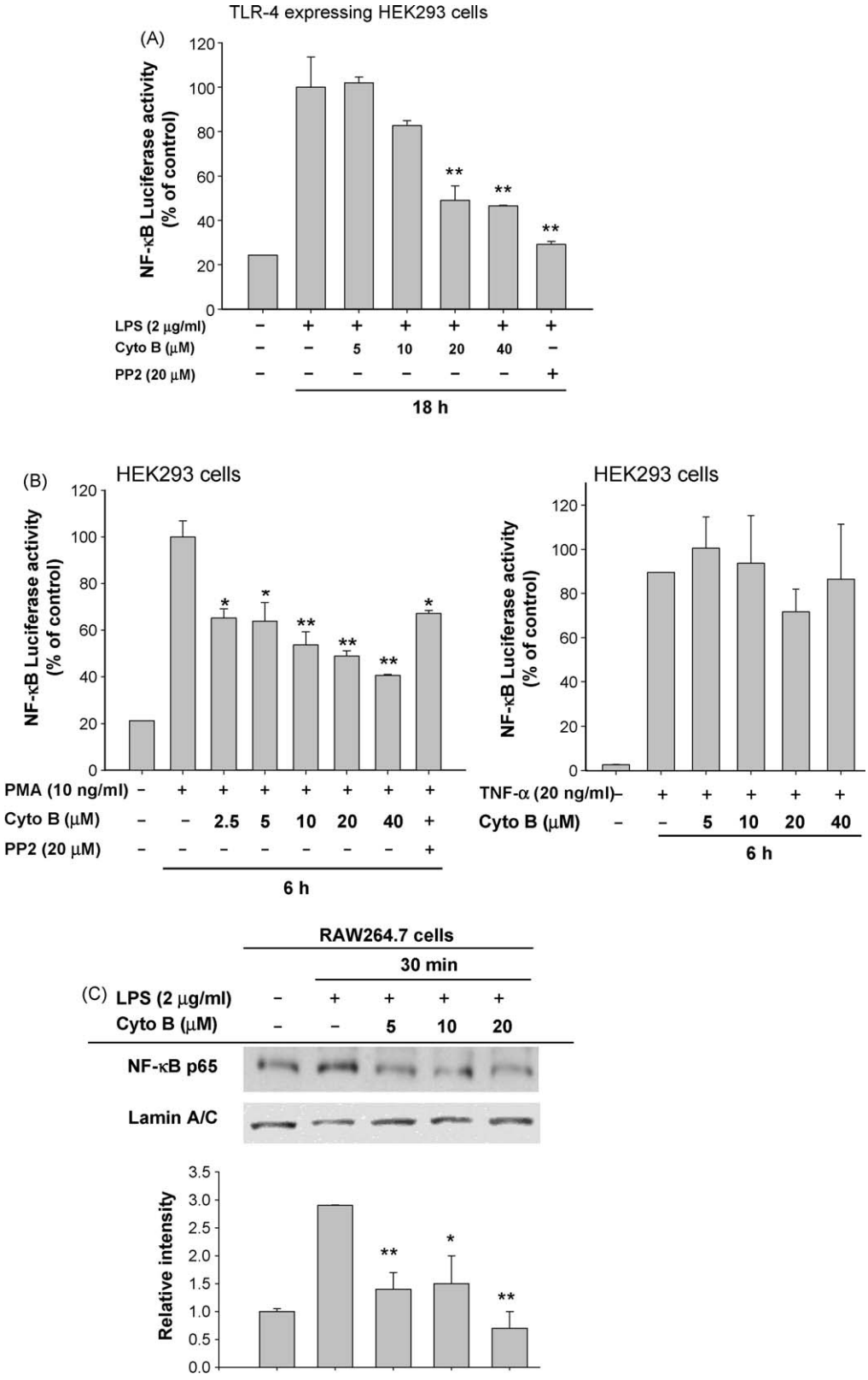

Fig. 4. The effect of cytochalasin B on NF-κB activation. (A an B) TLR4-expressing HEK293 cells transfected with plasmid constructs containing NF-κB-Luc (1 μg/ml each) as well as β-gal were treated with cytochalasin B or PP2 (a Src kinase inhibitor) in the presence or absence of LPS (2 μg/ml) (A), PMA (10 ng/ml) or TNF-α (20 ng/ml) (B) for indicated time. Luciferase activity was determined by luminometer as described in Section 2. Data represent the mean ± SEM of three independent experiments performed in triplicate. (C) RAW264.7 cells (5×10^6 cells/ml) were incubated with cytochalasin B in the presence or absence of LPS (2 μg/ml) for 30 min. Then, nuclear fraction was obtained from the cells, as described in Section 2. The nuclear levels of p65 and lamin A/C were determined by immunoblotting analysis. The results show one representative experiment of three. $^{*}p < 0.05$ and $^{**}p < 0.01$ compared to the control group.

tested. As Fig. 1B shows, this compound blocked NO production in a dose-dependent manner, indicating that actin polymerization is commonly required regardless of the cancerous state of the cells.

The NO inhibitory effect of cytochalasin B was not limited to TLR4-mediated signals. Thus, NO production induced by PGN, a TLR2 ligand, zymosan, β-glucans [curdlan, and fractions from *Tricholoma matsutake* (β-glucan I), and *Lentinus edodes* (β-glucan II)], dectin-1 ligands [25,26], was also strongly blocked by cytochalasin B (Fig. 1C). These results suggest that NO production in macrophages stimulated by various inflammatory stimuli may require actin cytoskeleton rearrangement.

3.2. Involvement of the actin cytoskeleton in LPS-induced PGE_2 and TNF-α production

Furthermore, to address whether actin disruption by cytochalasin B was able to diminish the production of other inflammatory mediators, the inhibitory potential of this compound on the production of PGE_2 and TNF-α was examined. As shown in Fig. 2, cytochalasin B strikingly suppressed the production of PGE_2 (Fig. 2A) and TNF-α (Fig. 2B) in LPS-treated RAW264.7 cells, indicating that cytochalasin B may possess broad-spectrum anti-inflammatory activity.

3.3. Cytochalasin B inhibition occurred at the transcriptional level of inflammatory genes

To elicit production of inflammatory mediators by macrophages, newly synthesized inducible proteins such as inflammatory enzymes are required. Therefore, we next examined whether cytochalasin B inhibited the transcriptional up-regulation of these genes by semi-quantitative RT-PCR. Fig. 3A shows that cytochalasin B was able to strongly suppress the mRNA expression of inflammatory enzymes such as iNOS, TNF-α and COX-2, suggesting that inhibition by cytochalasin B occurs at the transcriptional level. In particular, exposure to cytochalasin B 1 and 2 h after LPS, but not 1 h prior to LPS, failed to suppress iNOS expression (Fig. 3B), suggesting that the target of cytochalasin B appeared at early time points after LPS exposure. Similar inhibitory patterns (50–80% inhibition) of cytochalasin B on mRNA expression of these inflammatory genes were also obtained from quantitative real-time PCR analysis (Fig. 3C), although there was slight difference due to variability of Ct value in real-time profiling. Meanwhile, 3 h incubation condition of LPS displayed lower levels of iNOS expression than 6 h (Fig. 3B).

3.4. Inhibition of NF-κB activation is required for cytochalasin B-mediated inhibition of transcriptional activation

Based on previous papers showing that LPS activates a series of transcriptional factors, including NF-κB, necessary for the expression of inflammatory genes [27], we first investigated the transcription factor(s) targeted by cytochalasin B. To do this, we used a luciferase assay with plasmid construct composed of the binding promoter site for transcription factors NF-κB transfected into TLR4-expressing (Fig. 4A) or wild type HEK cells (Fig. 4B, left panel) under LPS, TNF-α, or PMA conditions. As expected, each stimulus enhanced the luciferase activity mediated by these transcription factors, and cytochalasin B suppressed NF-κB activity in a dose-dependent manner, as PP2 at non-cytotoxic concentration (20 μM) did. Interestingly, cytochalasin B did not block NF-κB-dependent luciferase activity in response to TNF-α treatment (Fig. 4B, right panel), suggesting that the actin cytoskeleton may modulate NF-κB activity in a stimulus-dependent manner. Consistent with this hypothesis, immunoblotting analysis provided similar results. Namely, nuclear fraction obtained after cytochalasin B treatment in the presence or absence of LPS exposure showed lowered level of translocated NF-κB/p65 in nuclei (Fig. 4C). In agreement, Fig. 5 strongly indicates that cytochalasin B, similar to PP2, blocked upstream events for NF-κB translocation such as LPS-induced phosphorylation of IKKβ at 5 min (Fig. 5A) and IκBα at 30 and 60 min (Fig. 5B), suggesting that cytochalasin B inhibited both NF-κB translocation and its upstream activation signals. The importance of NF-κB activation as an early event necessary for NO production was confirmed by treating cells with cytochalasin B (Fig. 3B) and

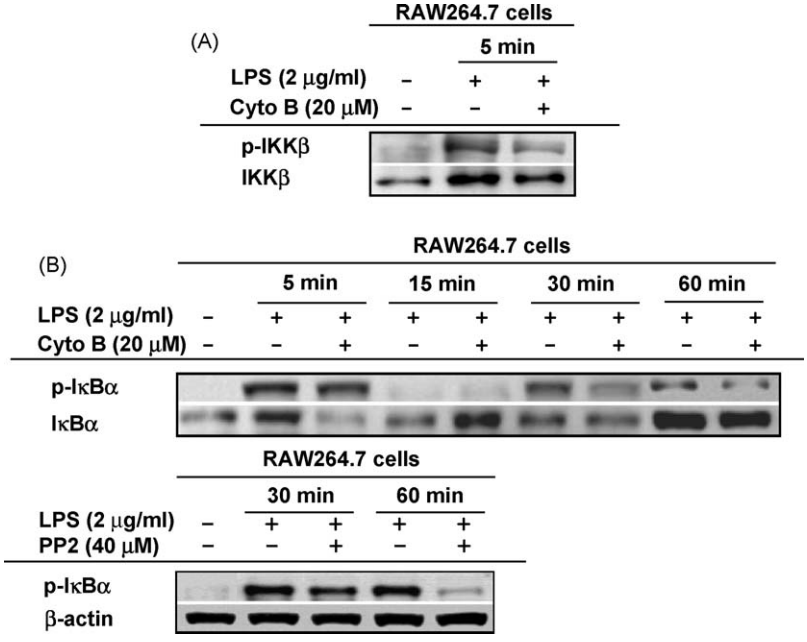

Fig. 5. The effect of cytochalasin B on NF-κB activation. (A and B) RAW264.7 cells (5×10^6 cells/ml) were stimulated with cytochalasin B or PP2 in the presence or absence of LPS (2 μg/ml). After immunoblotting, total or phospho-protein levels of IKKβ, IκBα, and β-actin were identified with their total protein- or phospho-specific antibodies. The results show one representative experiment of three.

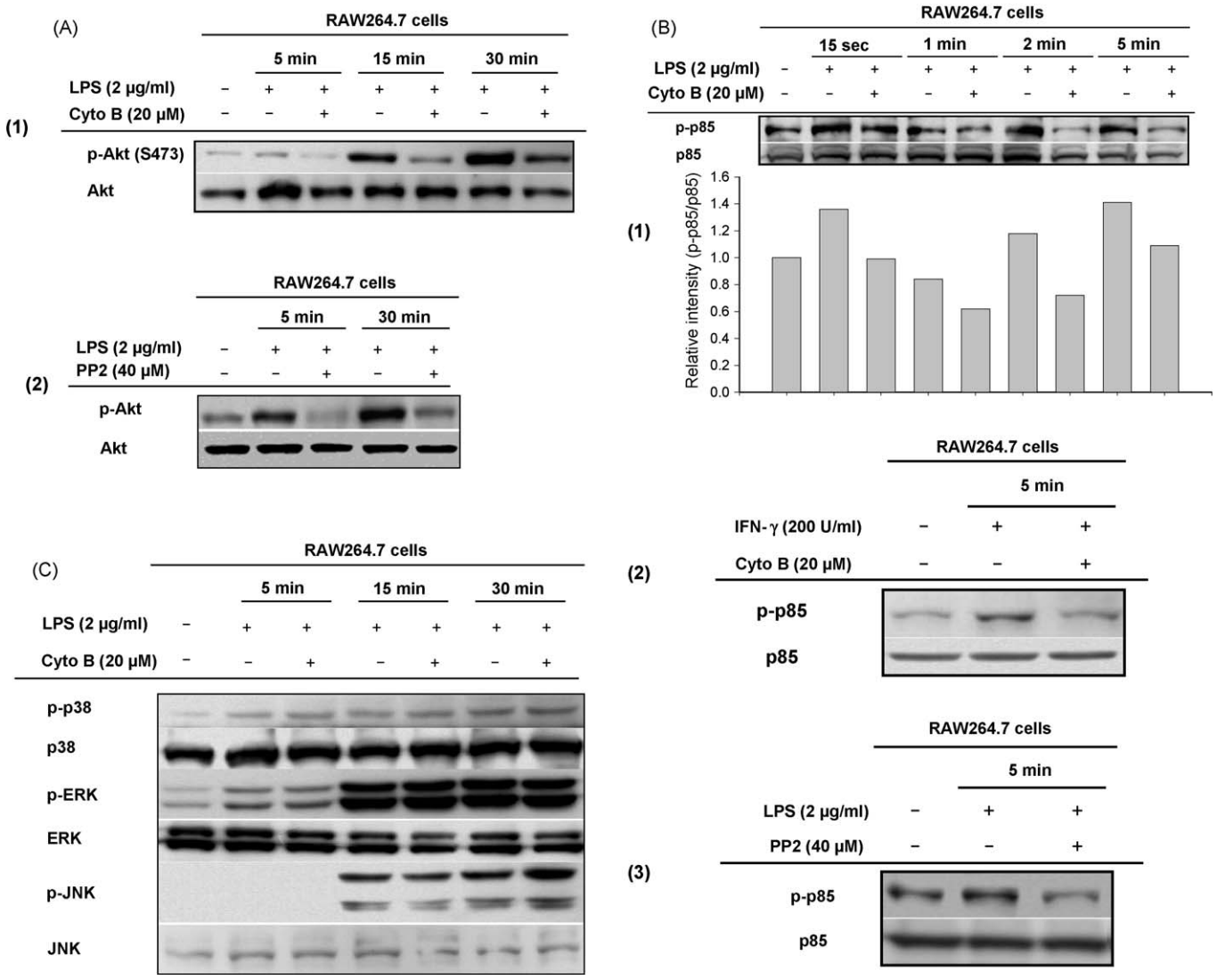

Fig. 6. The effect of cytochalasin B on the upstream signaling pathway leading to NF-κB activation. (A–C) RAW264.7 cells (5×10^6 cells/ml) were stimulated with cytochalasin B or PP2 in the presence or absence of LPS (2 μg/ml) or IFN-γ (200 U/ml). After immunoblotting, total or phospho-protein levels of Akt (A), p85 (B), MAPK (C), and β-actin were identified with their total protein- or phospho-specific antibodies. The results show one representative experiment of three.

selective NF-κB inhibitors [cynaropicrin (Cynar), BAY11-7082 (Bay11) and SN50] at different time points (Fig. S2). Thus, all NF-κB inhibitors strongly suppressed the production of NO from LPS-activated RAW264.7 cells (Fig. S2), as reported previously [21,28].

3.5. Cytochalasin B strongly inhibits the PI3K/Akt pathway necessary for NF-κB activation

Several upstream signaling cascades necessary for NF-κB activation have been reported thus far. To gain additional information as to whether cytochalasin B could modulate upstream signaling events, we evaluated its effect on the PI3K/Akt and MAPK pathways. phosphorylation of Akt (Fig. 6A) and p85/PI3K (a regulatory subunit of PI3K) (Fig. 6B1) was clearly decreased by cytochalasin B treatment compared with LPS alone, as observed for PP2 (Fig. 6B3). Furthermore, this compound also blocked the IFN-γ-stimulated phosphorylation of p85 (Fig. 6B2), suggesting that cytochalasin B may down-regulate the activity of some kinases involved in phosphorylating p85 and Akt under macrophage-activating conditions. In contrast, the LPS-induced phosphorylation of p38, ERK, and JNK was not diminished, and no alterations were observed in the total forms of MAPKs (Fig. 6C), indicating that these proteins were not affected by cytochalasin B treatment.

3.6. Actin cytoskeleton disruption by cytochalasin B is linked to impairment of Src activation

To elucidate the upstream target of cytochalasin B, therefore, the activation-related phosphorylation pattern of other non-receptor type tyrosine kinases (such as Syk, JAK-2, and Src) known to be upstream kinases responsible for PI3K activation, were examined. Indeed, we previously found that the phosphorylation of JAK-2, Src, and Syk was LPS-inducible at 1 and 2.5 min [29]. Interestingly, cytochalasin B blocked the LPS-induced phosphorylation of Src (Fig. 7A), while JAK-2 and Syk phosphorylation at 2.5 and 5 min was not diminished (Fig. S3). Non-pharmacological intervention of actin level by siActin also displayed very similar inhibitory pattern of Src phosphorylation (Fig. 7B), indicating that

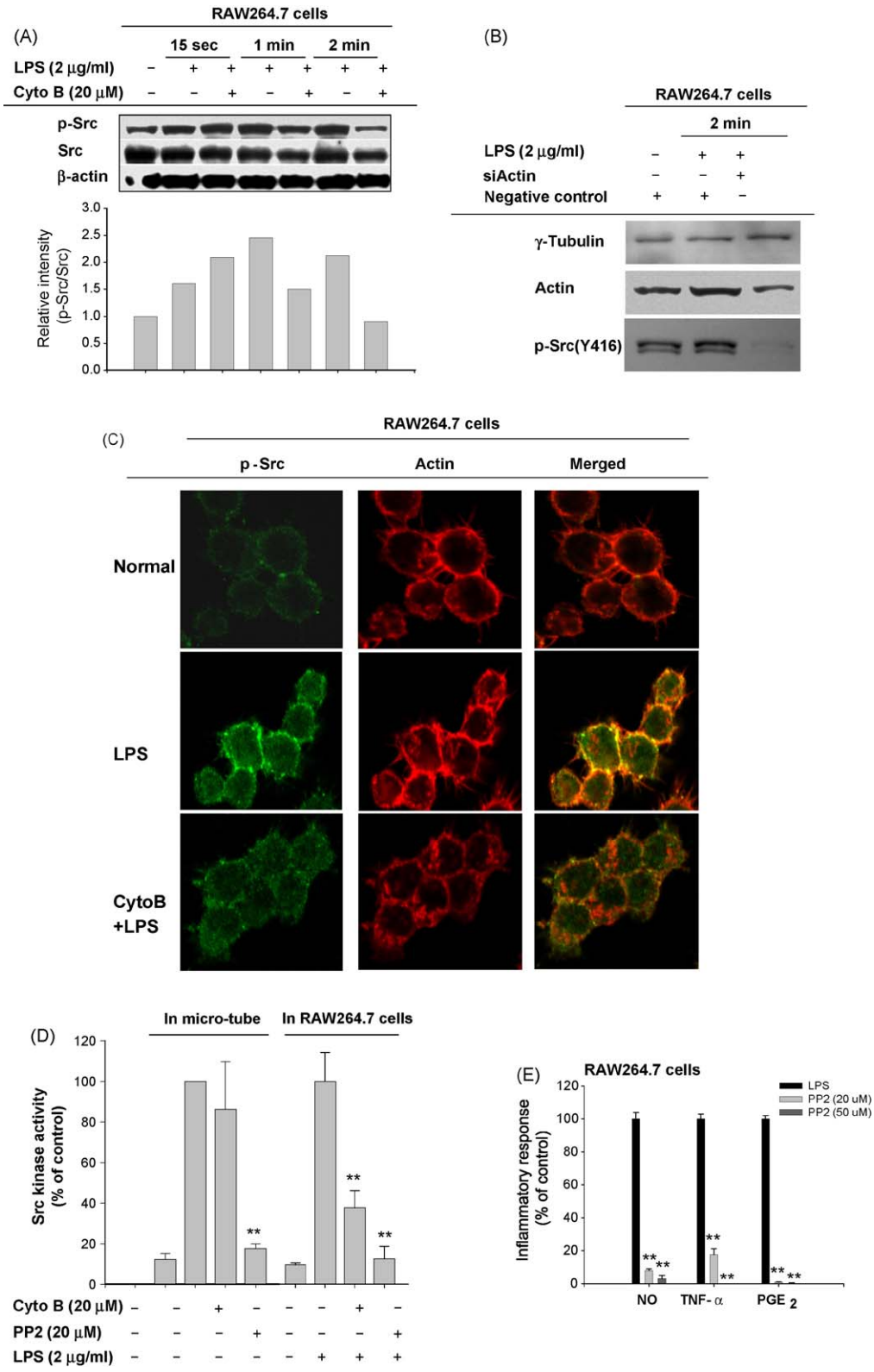

Fig. 7. The effect of cytochalasin B on the up-regulation of Src kinase activity. (A) RAW264.7 cells (5×10^6 cells/ml) were stimulated with cytochalasin B in the presence or absence of LPS (2 μg/ml). After immunoblotting, total or phospho-protein levels of Src were identified with their total protein- or phospho-specific antibodies. The results show one representative experiment of three. (B) siActin-treated RAW264.7 cells (5×10^6 cells/ml) were stimulated with cytochalasin B in the presence or absence of LPS (2 μg/ml). After immunoblotting, total or phospho-protein levels of Src, actin and γ-tubulin were identified with their total protein- or phospho-specific antibodies. The results show one representative experiment of three. (C) Confocal analysis of Src phosphorylation was performed using a method as described in Section 2. The results show one representative experiment of three. (D) Cytochalasin B was incubated either directly with immunoprecipitated Src (In microtube) for 10 min or used to treat RAW264.7 cells in the presence or absence of LPS (2 μg/ml) for 30 min (In RAW264.7 cells), and Src kinase activity was examined after immunoprecipation with anti-Src antibody according to the manufacturer's protocol. (E) RAW264.7 cells (1×10^6 cells/ml) were treated with PP2 in the presence or absence of LPS (2 μg/ml) for 6 (TNF-α) or 24 (NO and PGE_2) h. Supernatants were collected and NO, PGE_2 and TNF-α levels present in the supernatants were determined by Griess assay, EIA or ELISA as described in Section 2. Data represent the mean ± SEM of three independent observations performed in triplicate. $^{**}p < 0.01$ compared to the control.

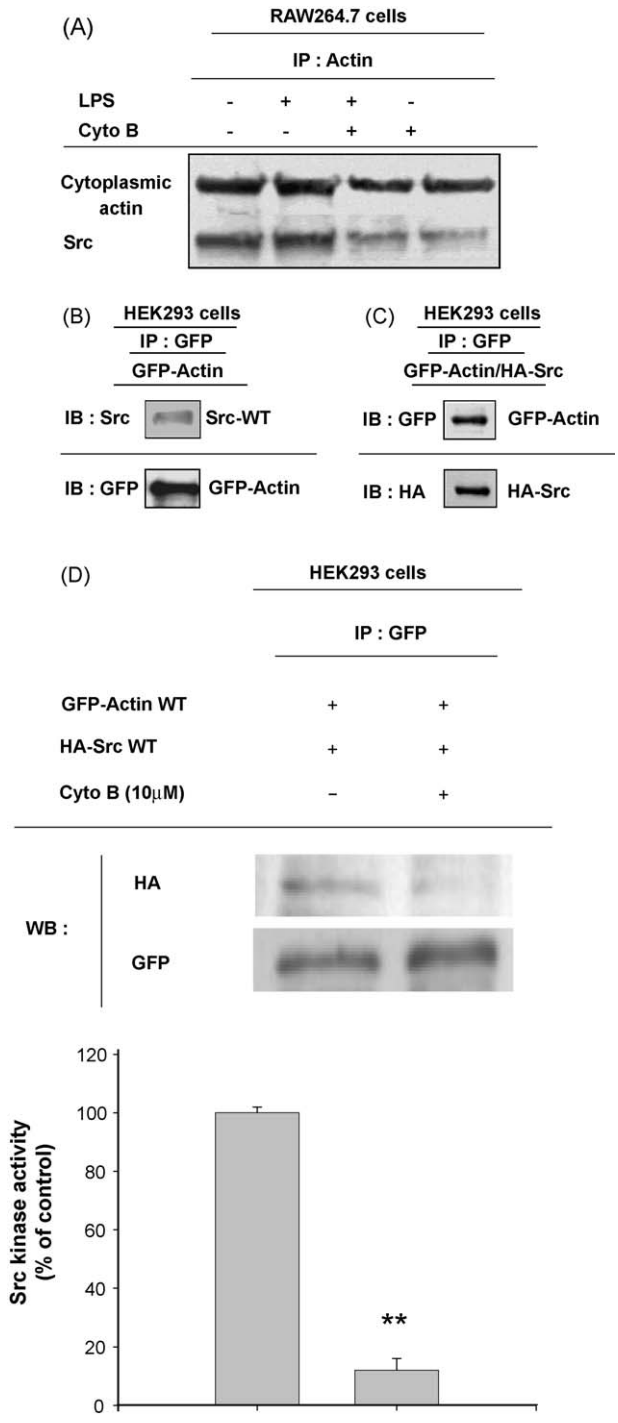

Fig. 8. Molecular characterization of the interaction between actin and Src. (A) RAW264.7 cells (1×10^7 cells/ml) were pre-treated with cytochalasin B in the presence or absence of LPS (2 μg/ml) for 30 min. Co-immunoprecipitation of Src with actin was determined by immunoprecipitation analysis as described in Section 2. (B) HEK cells (1×10^7 cells/ml) pre-treated with plasmid constructs containing GFP-actin-WT were lysed, and co-immunoprecipitation of Src with GFP-actin was determined by immunoprecipitation with anti-GFP antibody analysis as described in Section 2. (C) Association and expression levels of HA-tagged Src protein and GFP-actin were determined by immunoblotting with anti-HA and GFP antibodies from HEK cell lysates transfected with plasmid constructs containing GFP-actin-WT and HA-tagged Src-WT. (D) HEK cells (1×10^7 cells/ml) pre-treated with plasmid construct containing GFP-actin-WT in the presence or absence of cytochalasin B (10 μM) were lysed, and co-immunoprecipitation of Src with actin was determined by immunoprecipitation analysis as described in Section 2. Src kinase activity was also examined after immunoprecipation with anti-Src antibody according to the manufacturer's protocol.

there is no suppressive difference between pharmacological inhibition and knock-down of actin. Furthermore, cytochalasin B inhibition of LPS-induced phosphorylation of Src was also clearly seen by confocal microscopy (Fig. 7C). To address whether cytochalasin B directly blocked Src kinase activity, an enzyme assay was performed. As Fig. 7D shows, cytochalasin B did not directly block Src kinase activity when added to a microtube containing immunoprecipitated Src kinase, while PP2, a selective Src kinase inhibitor, strongly suppressed Src kinase activity. Interestingly, however, when cytochalasin B was incubated with RAW264.7 cells in the presence of LPS, Src activity was strongly diminished (Fig. 7D), suggesting that cytochalasin B indirectly blocked a Src kinase-related pathway. Meanwhile, the regulatory role of Src in the production of inflammatory mediators was also confirmed with PP2, a selective inhibitor of Src. Thus, PP2 completely blocked the production of NO, TNF-α, and PGE_2 (Fig. 7E).

3.7. Actin polymerization is a critical factor in the actin/Src association

To understand the regulatory mechanism by which the actin cytoskeleton modulates the activation of Src kinase, we focused on dissecting the molecular interaction between Src and actin. Thus, whether actin and Src were associated biochemically was carefully investigated. As Fig. 8A indicates, Src seemed to be constitutively associated with actin immunoprecipitated with cytoplasmic actin antibody regardless of LPS stimulation in RAW264.7 cells. However, actin disruption by cytochalasin B remarkably down-regulated the interaction of cytoplasmic actin and Src (Fig. 8A), suggesting that actin polymerization may boost the interaction between actin and Src. To further characterize the association between actin and Src, we transfected DNA constructs including GFP-fused actin and HA-tagged Src. In agreement with result obtained with RAW264.7 cells, GFP-fused actin was associated with endogenous Src (Fig. 8B) as well as transfected HA-tagged Src (Fig. 8C). Finally, to check whether polymerization of actin can affect the interaction between actin and Src, HEK cells cotransfected with GFP-actin and HA-Src constructs were incubated with cytochalasin B for 24 h and associated level of HA with immunoprecipitated GFP was evaluated. Interestingly, cytochalasin B strongly blocked biochemical association of Src and actin seen in normal cotransfection (Fig. 8D, Top panel) as well as Src kinase activity of this complex (Fig. 8D, bottom panel), suggesting that actin polymerization may be a critical event for molecular interaction of Src and actin.

4. Discussion

Actin cytoskeleton disruption by cytochalasin B down-regulated inflammatory events in activated macrophages without affecting cell viability, in agreement with previous results obtained with cytochalasin D [16]. Thus, the decrease in inflammatory parameter production (e.g., NO release [Fig. 1A], TNF-α secretion [Fig. 2A], and PGE_2 production [Fig. 2B]) implied the critical role of actin polymerization in inflammatory responses in macrophages. Inhibition of LPS signaling by actin cytoskeleton disruption was also reported in other cell types such as small intestinal lamina propria fibroblasts [30], pneumocytes [31], neutrophils [32], and vascular smooth muscle cells [33]. Furthermore, our results indicate a broad role of actin polymerization in regulating cellular functions of other PRRs, responsive to various external ligands such as β-glucan, peptidoglycan, and zymosan (Fig. 1C). In terms of inhibitory potency, the effects of cytochalasin B (IC_{50} values = 2–10 μM) on inflammatory mediator production were comparable to other anti-inflammatory drugs such as curcumin [23], and higher than those of gomisin A,

genipin, pentoxifylline, theophylline, and petrocortyne A [34–36]. Hence, actin cytoskeleton-regulating drugs may be regarded as promising anti-inflammatory agents.

Transcriptional control of inflammatory genes is known to be managed by redox-sensitive transcription factors such as NF-κB and AP-1 [37]. Disruption of the actin cytoskeleton by cytochalasin D and latrunculin B without PRR ligand treatment is reported to induce NF-κB activation via Nod2 protein and to produce IL-8 in various monocytic cells via reactive oxygen species (ROS) [38,39]. Contrastly, it was obtained that cytochalasin B treated with LPS, a TLR4 ligand, or PMA suppressed the transcriptional activation [NF-κB (Fig. 4A and B, left panel) and AP-1 (Fig. S4)] of inflammatory mediators, according to a reporter gene assay with wild type or TLR4-expressing HEK293 cells, as reported previously [23,40,41]. Interestingly, TNF-α-mediated NF-κB activation was not decreased by cytochalasin B (Fig. 4B, right panel), suggesting that cytochalasin-mediated inhibition of redox-sensitive transcription factors (NF-κB and AP-1) may be variable by the treatment of stimuli as well as cell types. The inhibition of NF-κB-mediated luciferase activity was also confirmed by immunoblotting analysis. Thus, cytochalasin B also blocked both the phosphorylation of IKK and IκBα (Fig. 5) as well as the nuclear translocation of p65/NF-κB (Fig. 4C). The facts that it did not have a direct radical scavenging effect (Fig. S5) and cytochalasin B lost its NF-κB inhibitory activity during TNF-α stimulation (Fig. 4B, right panel) suggest indirect inhibition of transcriptional activation by actin cytoskeleton disruption as pointed out previously [42].

So far, it is not yet clear how upstream kinases phosphorylate the regulatory subunit, p85, a regulatory subunit of PI3K to activate a series of intracellular signaling cascade composed of PDK1, Akt and IKK/IκBα [43], during LPS stimulation. JAK-2, Src, and Syk are known as candidate tyrosine kinases for the phosphorylation of p85 during LPS exposure [44,45]. Therefore, whether actin cytoskeleton disruption by cytochalasin B was able to modulate the activity of p85/PI3K-phosphorylating enzymes was explored. Several lines of evidence strongly support that Src kinase is a target of actin polymerization. First, cytochalasin B blocked Src phosphorylation induced by LPS treatment at 1, 2, and 5 min and Src kinase activity in treated RAW264.7 cells according to immunoblotting analysis (Fig. 7A), confocal microscopy (Fig. 7C), and the Src kinase assay (Fig. 7D), although it did not directly block Src kinase activity, unlike PP2 (Fig. 7D). Second, the inhibitory pattern of the phosphorylation levels of p85, Akt, and IκBα as well as the luciferase activities (Figs. 4A, 5 and 6B) in response to cytochalasin B were very similar to that obtained using PP2.

Src kinase has been shown to play a central role in mediating inflammatory responses elicited by LPS. Src involvement in this pathway has been demonstrated using a variety of cell types (including monocytes and macrophages) and examining several inflammatory parameters (including NO and TNF-α) [46–49]. LPS treatment increased the activation of Src and Src family kinases such as Hck, Lyn, Yes, and Fyn, as assessed by measuring phosphorylation levels and kinase activities [50]. Indeed, strong inhibitors of Src family kinases (PP1 and PP2) were clearly shown to block LPS-induced inflammatory events [46,48]. Nonetheless, the molecular association of Src and actin is not fully understood. Controversial points are whether Src can act centrally as an actin cytoskeleton regulator or whether actin (in particular, polymerized actin) is the real player necessary for Src kinase activation. Even though Src critically modulates the actin cytoskeleton linked to morphological changes and cell mobility [51,52], and actin is phosphorylated by Src [51], inter-regulatory mechanisms between Src and actin are not clearly understood in macrophage-mediated inflammatory responses.

It is found that actin disruption by cytochalasin B or knockdown of actin by siRNA was strongly found to defect the phosphorylation of Src and its kinase activity during LPS treatment (Fig. 7A, B and D), implying that actin seems to be an upper regulator of Src kinase activation. Furthermore, cytochalasin B treatment decreased the molecular binding between Src and actin (Fig. 8A–C). The molecular association of Src and actin has been found to be managed in a SH2-domain dependent manner by using deletion mutants of HA-Src (Lee and Cho, unpublished data). More interestingly, unpolymerized condition of transfected GFP-actin induced by long exposure of cytochalasin B severely damaged the binding of Src to actin (Fig. 8D, top panel) and its kinase activity (Fig. 8D, bottom panel). Moreover, an actin mutant (GFP-actin H72A) with a deficiency in actin polymerization by replacing histidine 72, an important amino acid site for actin polymerization via methylation [53,54], to alanine was unable to bind to Src (Yoo, Lee, and Cho, unpublished data). Therefore, our data strongly suggest that polymerized actin could much play a critical role in modulating Src kinase activity as well as Src-mediated inflammatory events.

Unlike our data, the up-regulation of NF-κB by cytochalasin D was found in human intestinal epithelial cells and monocytic cells [38,55,56]. So far, we cannot exactly explain why there is a discrepancy between our data and previous reports [38,55,56]. Considering that a tight functional interaction between actin cytoskeleton and ROS-generating NADPH oxidase, responsible for NF-κB (as well as its upstream signaling enzyme) activating ROS generation, was observed in monocytes [7,38], Such difference between macrophages and other cells seems to be related to ROS generation system and cytoskeleton distribution pattern in each cell type. For this point, whether ROS generated in LPS-activated macrophages is really important for inhibiting or activating NF-κB and its upstream signaling pathways should be considered mainly to explain such discrepancy. ROS has been previously suggested to play a critical role in activation of redox-sensitive transcription factor such as NF-κB and AP-1 [57]. In spite of this notion, we and other group could not observe a strong relevance of ROS release in inhibition or activation of NO and PGE_2 production under LPS activation conditions. Thus, it was found that α-tocopherol, a strong antioxidant, did not block NF-κB activation and NO production, under concentrations with strong antioxidative property [58]. Anti-inflammatory function of antioxidants has been reported to be due to the activity blockade of inflammatory signaling enzymes such as Src [59] rather than a direct neutralizing effect of radicals generated, implying that ROS does not critically affect LPS-mediated inflammatory responses in macrophages. In view of this, it is speculated that the up-regulation does not affect the functional activation of macrophages, even though actin disruptors are able to increase ROS levels. To prove this possibility, detailed studies will be continued in the next experiments.

In summary, we found that cytochalasin B was able to down-regulate macrophage-mediated inflammatory responses such as NO production, PGE_2 release, and TNF-α secretion from macrophage-like RAW264.7 cells and primary peritoneal macrophages in a transcription level-dependent manner. Actin disruption blocked a series of signaling cascades such as of PI3K, Akt and IKK/IκBα necessary for NF-κB activation. The inhibition of Src phosphorylation and its kinase activity as well as molecular association of actin and Src by cytochalasin B suggests that Src is a potential downstream target of actin polymerization. Therefore, our data suggest that the actin cytoskeleton may play a central role in modulating inflammatory responses via regulation of Src kinase activity as summarized in Fig. 9.

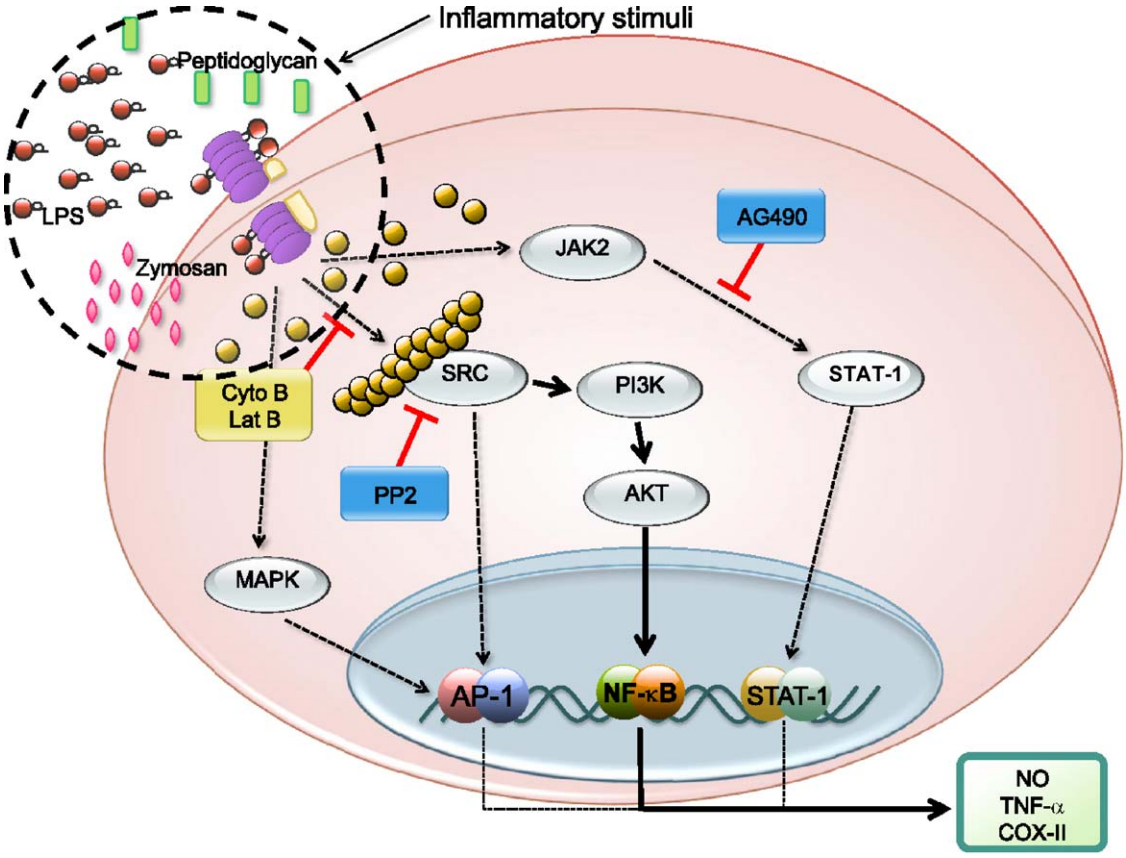

Fig. 9. Schematic regulatory role of actin cytoskeleton during inflammatory responses.

Acknowledgements

We acknowledge The Central Laboratory of Kangwon National University for allowing us to use their FACScan, and the Korea Basic Science Institute (Chuncheon) for help with the confocal experiments. This work was supported by a grant (2009-0073604) from NRF, Korea (to J.Y.C.).

Appendix A. Supplementary data

Supplementary data associated with this article can be found, in the online version, at doi:10.1016/j.bcp.2009.09.016.

References

[1] Qureshi N, Vogel SN, Van Way 3rd C, Papasian CJ, Qureshi AA, Morrison DC. The proteasome: a central regulator of inflammation and macrophage function. Immunol Res 2005;31:243–60.
[2] Malyshev IY, Shnyra A. Controlled modulation of inflammatory, stress and apoptotic responses in macrophages. Curr Drug Targets Immune Endocr Metabol Disord 2003;3:1–22.
[3] Palaniyar N, Nadesalingam J, Reid KB. Pulmonary innate immune proteins and receptors that interact with gram-positive bacterial ligands. Immunobiology 2002;205:575–94.
[4] Butchar JP, Parsa KV, Marsh CB, Tridandapani S. Negative regulators of toll-like receptor 4-mediated macrophage inflammatory response. Curr Pharm Des 2006;12:4143–53.
[5] Yoshimura A. Signal transduction of inflammatory cytokines and tumor development. Cancer Sci 2006;97:439–47.
[6] Kobori M, Yoshida M, Ohnishi-Kameyama M, Shinmoto H. Ergosterol peroxide from an edible mushroom suppresses inflammatory responses in RAW264.7 macrophages and growth of HT29 colon adenocarcinoma cells. Br J Pharmacol 2007;150:209–19.
[7] Kustermans G, Piette J, Legrand-Poels S. Actin-targeting natural compounds as tools to study the role of actin cytoskeleton in signal transduction. Biochem Pharmacol 2008;76:1310–22.
[8] Disanza A, Steffen A, Hertzog M, Frittoli E, Rottner K, Scita G. Actin polymerization machinery: the finish line of signaling networks, the starting point of cellular movement. Cell Mol Life Sci 2005;62:955–70.
[9] Perri SR, Annabi B, Galipeau J. Angiostatin inhibits monocyte/macrophage migration via disruption of actin cytoskeleton. FASEB J 2007;21:3928–36.
[10] Shimada O, Ishikawa H, Tosaka-Shimada H, Atsumi S. Rearrangements of actin cytoskeleton during infection with *Escherichia coli* O157 in macrophages. Cell Struct Funct 1999;24:237–46.
[11] Araki N. Role of microtubules and myosins in Fc gamma receptor-mediated phagocytosis. Front Biosci 2006;11:1479–90.
[12] Tabas I, Zha X, Beatini N, Myers JN, Maxfield FR. The actin cytoskeleton is important for the stimulation of cholesterol esterification by atherogenic lipoproteins in macrophages. J Biol Chem 1994;269:22547–56.
[13] Zeng C, Morrison AR. Disruption of the actin cytoskeleton regulates cytokine-induced iNOS expression. Am J Physiol Cell Physiol 2001;281:C932–40.
[14] Daniliuc S, Bitterman H, Rahat MA, Kinarty A, Rosenzweig D, Lahat N. Hypoxia inactivates inducible nitric oxide synthase in mouse macrophages by disrupting its interaction with alpha-actinin 4. J Immunol 2003;171:3225–32.
[15] Szabo G, Dolganiuc A, Dai Q, Pruett SB. TLR4, ethanol, and lipid rafts: a new mechanism of ethanol action with implications for other receptor-mediated effects. J Immunol 2007;178:1243–9.
[16] Shinji H, Akagawa KS, Yoshida T. Cytochalasin D inhibits lipopolysaccharide-induced tumor necrosis factor production in macrophages. J Leukoc Biol 1993;54:336–42.
[17] Azim AC, Cao H, Gao X, Joo M, Malik AB, van Breemen RB, et al. Regulation of cyclooxygenase-2 expression by small GTPase Rac2 in bone marrow macrophages. Am J Physiol Lung Cell Mol Physiol 2007;293:L668–73.
[18] Zaru R, Mollahan P, Watts C. PDK1 deficiency perturbs toll-like receptor signalling events and actin cytoskeleton dynamics in dendritic cells. J Biol Chem 2007.
[19] Gevrey JC, Isaac BM, Cox D. Syk is required for monocyte/macrophage chemotaxis to CX3CL1 (Fractalkine). J Immunol 2005;175:3737–45.
[20] Yang KJ, Shin S, Piao L, Shin E, Li Y, Park KA, et al. Regulation of 3-phosphoinositide-dependent protein kinase-1 (PDK1) by Src involves tyrosine phosphorylation of PDK1 and Src homology 2 domain binding. J Biol Chem 2008;283:1480–91.
[21] Cho JY, Baik KU, Jung JH, Park MH. In vitro anti-inflammatory effects of cynaropicrin, a sesquiterpene lactone, from Saussurea lappa. Eur J Pharmacol 2000;398:399–407.
[22] Cho JY, Park JS, Baik KU, Lee JG, Kim HP, Yoo ES, et al. Differential effect of phosphodiesterase IV inhibitor RP73401 on various inflammatory and

immune responses relevant to rheumatoid arthritis. Pharmacol Res 2004;49:423–31.
[23] Jung KK, Lee HS, Cho JY, Shin WC, Rhee MH, Kim TG, et al. Inhibitory effect of curcumin on nitric oxide production from lipopolysaccharide-activated primary microglia. Life Sci 2006;79:2022–31.
[24] Byeon SE, Lee YG, Kim BH, Shen T, Lee SY, Park HJ, et al. Surfactin blocks NO production in lipopolysaccharide-activated macrophages by inhibiting NF-kappaB activation. J Microbiol Biotechnol 2008;18:1984–9.
[25] Kim JY, Byeon SE, Lee YG, Lee JY, Park J, Hong EK, et al. Immunostimulatory activities of polysaccharides from liquid culture of pine-mushroom *Tricholoma matsutake*. J Microbiol Biotechnol 2008;18:95–103.
[26] Lee JY, Kim JY, Lee YG, Rhee MH, Hong EK, Cho JY. Molecular mechanism of macrophage activation by exopolysaccharides from liquid culture of lentinus edodes. J Microbiol Biotechnol 2008;18:355–64.
[27] Evans SE, Hahn PY, McCann F, Kottom TJ, Pavlovic ZV, Limper AH. Pneumocystis cell wall beta-glucans stimulate alveolar epithelial cell chemokine generation through nuclear factor-kappaB-dependent mechanisms. Am J Respir Cell Mol Biol 2005;32:490–7.
[28] Hong J, Yokomakura A, Nakano Y, Ban HS, Ishihara K, Ahn JW, et al. Induction of nitric oxide production by the cytostatic macrolide apicularen A [2,4-heptadienamide, N-[(1E)-3-[(3S,5R,7R,9S)-3,4,5,6,7,8,9,10-octahydro-7,14 dihydroxy-1-oxo-5,9-epoxy-1H-2-benzoxacyclododecin-3-yl]-1 propenyl]-, (2Z,4Z)-(9CI)] and possible role of nitric oxide in apicularen A-induced apoptosis in RAW 264. 7 cells. J Pharmacol Exp Ther 2005;312:968–77.
[29] Lee YG, Chain BM, Cho JY. Distinct role of spleen tyrosine kinase in the early phosphorylation of inhibitor of kappaB alpha via activation of the phosphoinositide-3-kinase and Akt pathways. Int J Biochem Cell Biol 2009;41:811–21.
[30] Chakravortty D, Nanda Kumar KS. Bacterial lipopolysaccharide induces cytoskeletal rearrangement in small intestinal lamina propria fibroblasts: actin assembly is essential for lipopolysaccharide signaling. Biochim Biophys Acta 2000;1500:125–36.
[31] Isowa N, Liu M. Role of LPS-induced microfilament depolymerization in MIP-2 production from rat pneumocytes. Am J Physiol Lung Cell Mol Physiol 2001;280:L762–770.
[32] Howard TH, Wang D, Berkow RL. Lipopolysaccharide modulates chemotactic peptide-induced actin polymerization in neutrophils. J Leukoc Biol 1990; 47:13–24.
[33] Kato T, Hashikabe H, Iwata C, Akimoto K, Hattori Y. Statin blocks Rho/Rho-kinase signalling and disrupts the actin cytoskeleton: relationship to enhancement of LPS-mediated nitric oxide synthesis in vascular smooth muscle cells. Biochim Biophys Acta 2004;1689:267–72.
[34] Lim H, Park KR, Lee DU, Kim YS, Kim HP. Effects of the constituents of gardenia fructus on prostaglandin and NO production. Biomol Therapeut 2008;16:82–6.
[35] Choi MS, Kwon KJ, Jeon SJ, Go HS, Kim KC, Ryu JR, et al. Schizandra chinesis alkaloids inhibit lipopolysaccharide-induced inflammatory responses in BV2 microglial cells. Biomol Therapeut 2009;17:47–56.
[36] Hong S, Kim SH, Rhee MH, Kim AR, Jung JH, Chun T, et al. In vitro anti-inflammatory and pro-aggregative effects of a lipid compound, petrocortyne A, from marine sponges. Naunyn Schmiedebergs Arch Pharmacol 2003; 368:448–56.
[37] Hardy K, Hunt NH. Effects of a redox-active agent on lymphocyte activation and early gene expression patterns. Free Radic Biol Med 2004;37:1550–63.
[38] Kustermans G, El Benna J, Piette J, Legrand-Poels S. Perturbation of actin dynamics induces NF-kappaB activation in myelomonocytic cells through an NADPH oxidase-dependent pathway. Biochem J 2005;387:531–40.
[39] Legrand-Poels S, Kustermans G, Bex F, Kremmer E, Kufer TA, Piette J. Modulation of Nod2-dependent NF-kappaB signaling by the actin cytoskeleton. J Cell Sci 2007;120:1299–310.
[40] Hirota K, Matsui M, Murata M, Takashima Y, Cheng FS, Itoh T, et al. Nucleoredoxin, glutaredoxin, and thioredoxin differentially regulate NF-kappaB, AP-1, and CREB activation in HEK293 cells. Biochem Biophys Res Commun 2000;274:177–82.
[41] Latz E, Visintin A, Lien E, Fitzgerald KA, Espevik T, Golenbock DT. The LPS receptor generates inflammatory signals from the cell surface. J Endotoxin Res 2003;9:375–80.
[42] Ingram DA, Forman MB, Murray JJ. Phagocytic activation of human neutrophils by the detergent component of fluosol. Am J Pathol 1992;140:1081–7.
[43] Okkenhaug K, Vanhaesebroeck B. New responsibilities for the PI3K regulatory subunit p85 alpha. Sci STKE 2001;2001:PE1.
[44] Moissoglu K, Sachdev S, Gelman IH. Enhanced v-Src-induced oncogenic transformation in the absence of focal adhesion kinase is mediated by phosphatidylinositol 3-kinase. Biochem Biophys Res Commun 2005;330:673–84.
[45] Park J, Hill MM, Hess D, Brazil DP, Hofsteenge J, Hemmings BA. Identification of tyrosine phosphorylation sites on 3-phosphoinositide-dependent protein kinase-1 and their role in regulating kinase activity. J Biol Chem 2001; 276:37459–71.
[46] Lee HS, Moon C, Lee HW, Park EM, Cho MS, Kang JL. Src tyrosine kinases mediate activations of NF-kappaB and integrin signal during lipopolysaccharide-induced acute lung injury. J Immunol 2007;179:7001–11.
[47] Smolinska MJ, Horwood NJ, Page TH, Smallie T, Foxwell BM. Chemical inhibition of Src family kinases affects major LPS-activated pathways in primary human macrophages. Mol Immunol 2008;45:990–1000.
[48] Lee JY, Lowell CA, Lemay DG, Youn HS, Rhee SH, Sohn KH, et al. The regulation of the expression of inducible nitric oxide synthase by Src-family tyrosine kinases mediated through MyD88-independent signaling pathways of Toll-like receptor 4. Biochem Pharmacol 2005;70:1231–40.
[49] Leu TH, Charoenfuprasert S, Yen CK, Fan CW, Maa MC. Lipopolysaccharide-induced c-Src expression plays a role in nitric oxide and TNFalpha secretion in macrophages. Mol Immunol 2006;43:308–16.
[50] Khadaroo RG, Kapus A, Powers KA, Cybulsky MI, Marshall JC, Rotstein OD. Oxidative stress reprograms lipopolysaccharide signaling via Src kinase-dependent pathway in RAW 264.7 macrophage cell line. J Biol Chem 2003;278:47834–41.
[51] Avizienyte E, Keppler M, Sandilands E, Brunton VG, Winder SJ, Ng T, et al. An active Src kinase-beta-actin association is linked to actin dynamics at the periphery of colon cancer cells. Exp Cell Res 2007;313:3175–88.
[52] Kilarski WW, Jura N, Gerwins P. Inactivation of Src family kinases inhibits angiogenesis in vivo: implications for a mechanism involving organization of the actin cytoskeleton. Exp Cell Res 2003;291:70–82.
[53] Kalhor HR, Niewmierzycka A, Faull KF, Yao X, Grade S, Clarke S, et al. A highly conserved 3-methylhistidine modification is absent in yeast actin. Arch Biochem Biophys 1999;370:105–11.
[54] Yao X, Grade S, Wriggers W, Rubenstein PA. His(73), often methylated, is an important structural determinant for actin. A mutagenic analysis of HIS(73) of yeast actin. J Biol Chem 1999;274:37443–9.
[55] Nemeth ZH, Deitch EA, Davidson MT, Szabo C, Vizi ES, Hasko G. Disruption of the actin cytoskeleton results in nuclear factor-kappaB activation and inflammatory mediator production in cultured human intestinal epithelial cells. J Cell Physiol 2004;200:71–81.
[56] Kustermans G, El Mjiyad N, Horion J, Jacobs N, Piette J, Legrand-Poels S. Actin cytoskeleton differentially modulates NF-kappaB-mediated IL-8 expression in myelomonocytic cells. Biochem Pharmacol 2008;76:1214–28.
[57] Lee CH, Kim SY. NF-kappaB and therapeutic approach. Biomol Therapeut 2009;17:219–40.
[58] Jung WJ, Sung MK. Effects of major dietary antioxidants on inflammatory markers of RAW 264.7 macrophages. Biofactors 2004;21:113–7.
[59] Lee YG, Lee WM, Kim JY, Lee JY, Lee IK, Yun BS, et al. Src kinase-targeted anti-inflammatory activity of davallialactone from *Inonotus xeranticus* in lipopolysaccharide-activated RAW264.7 cells. Br J Pharmacol 2008;154: 852–63.